For negative ions such as N^{3-} or O^{2-}, however, the form factors obtained by the Watson-sphere model deviate significantly from renormalized values, which do not account for changes in the wave functions between the negative ion and the neutral atom. However, the valence wave functions and consequently the total form factor (mainly for small $\sin\theta/\lambda$ values) depend on the Watson-sphere radius and therefore on the crystalline environment. Thus there is not just *one* form factor for a negative ion, but a variation with r_W. The importance of this variation is demonstrated in the structure investigation of Li_3N in the following paper.

In the calculation of scattering factors for C the $X\alpha_{vt}$ method has been found (§ 3) to be accurate to about 1%. This seems to be sufficiently accurate for the present work, since we discuss larger differences. Recently, however, in connection with a study of the ionization potentials of atoms, it has been pointed out (Schwarz, 1978) that there is a fundamental difference between the HF and $X\alpha$ methods in that the instability for free negative ions is always found at smaller ionicities in the $X\alpha$ method (leading to more diffuse wave functions) than is the case with HF theory. [A similar statement has been made for H^- by Shore, Rose & Zaremba (1977).] The stabilization of the negative ions provided by the Watson sphere makes this problem less critical here. In addition it seems likely that a small reduction of r_W (*i.e.* an increasing stabilization) will effectively compensate for this difference between the $X\alpha$ and HF wave functions to a large extent.

The authors are pleased to acknowledge valuable discussions with Dr H. Völlenkle. All calculations were carried out at the Rechenzentrum der Technischen Universität Wien.

References

BROWN, R. T. (1971). *J. Chem. Phys.* **55**, 353–355.

CROMER, D. T. & MANN, J. B. (1968). *Acta Cryst.* A**24**, 321–324.

FRAGA, S., KARWOWSKI, J. & SAXENA, K. M. S. (1976). *Handbook of Atomic Data*. Amsterdam: Elsevier.

HEDIN, L. & LUNDQVIST, S. (1972). *J. Phys. (Paris) Colloq.* **33**(3), 73–81.

HERMAN, F. & SKILLMAN, S. (1963). *Atomic Structure Calculations*. Englewood Cliffs, New Jersey: Prentice Hall.

PAULING, L. (1960). *The Nature of the Chemical Bond*, 3rd ed., pp. 228, 514. Ithaca: Cornell Univ. Press.

SCHULZ, H. & SCHWARZ, K. (1978). *Acta Cryst.* A**34**, 999–1005.

SCHWARZ, K. (1972). *Phys. Rev. B*, **5**, 2466–2468.

SCHWARZ, K. (1978). *J. Phys. B*, **11**, 1339–1351.

SHORE, H. B., ROSE, J. H. & ZAREMBA, E. (1977). *Phys. Rev. B*, **15**, 2858–2861.

SLATER, J. C. (1951). *Phys. Rev.* **81**, 385–390.

SUZUKI, T. (1960). *Acta Cryst.* **13**, 279.

TOKONAMI, M. (1965). *Acta Cryst.* **19**, 486.

WATSON, R. E. (1958). *Phys. Rev.* **111**, 1108–1110.

Acta Cryst. (1978). A**34**, 999–1005

Is there an N^{3-} Ion in the Crystal Structure of the Ionic Conductor Lithium Nitride (Li_3N)?

BY HEINZ SCHULZ

Max-Planck-Institut für Festkörperforschung, 7000 Stuttgart 80, Büsnauer Strasse 171, Federal Republic of Germany

AND KARLHEINZ SCHWARZ

Institut für Technische Elektrochemie, Technische Universität Wien, A-1060 Vienna, Getreidemarkt 9, Austria

(*Received* 23 *March* 1978; *accepted* 14 *June* 1978)

The structure parameters of Li_3N in the temperature range −120 to 20 °C were refined both for neutral atoms (Li^0 and N^0) and for ions (Li^+ and N^{3-}). For N^{3-} new scattering curves were used which were calculated by applying stabilizing Watson-sphere potentials for different radii. All structure parameters depend critically on the scattering curves used. However, only on the assumption of ions, and only for N^{3-} scattering curves corresponding to a small range of Watson radii, were physically meaningful structure parameters and R values down to 0·9% obtained. These structure refinements demonstrate that Li_3N can be considered as an ionic crystal in which the N^{3-} ion, though unstable as a free ion, is stabilized by the surrounding Li^+ ions.

1. Introduction

The crystal structure of lithium nitride, Li_3N, was first derived from the cubic ammonia structure (Brill, 1927). Later, Zintl & Brauer (1935) proposed a hexagonal structure model in space group *P6/mmm*, in which the N atoms are surrounded by eight Li atoms in the form of a hexagonal bipyramid (Fig. 1). The structure may also be described as a layer structure with Li_2N and Li layers perpendicular to **c**. Within the Li_2N layers each N and Li atom forms six and three Li–N bonds respectively. These layers are connected with each other by only one N–Li–N bond per elementary cell; this coincides in length and direction with the *c* axis.

Five space groups have Laue symmetry *6/mmm*; some of these allow a decrease of the crystal symmetry by small deviations from the atomic positions proposed by Zintl & Brauer (1935). Owing to the limited accuracy of their diffraction data, it was impossible to resolve such deviations and to ensure the correct space group. Therefore, a reinvestigation of the structure was carried out by Rabenau & Schulz (1976); this confirmed the space group and the structural model of Zintl & Brauer (1935).

The nature of the bonding in Li_3N has long been a subject of dispute. Zintl & Brauer (1935) concluded from crystal-chemical considerations that Li_3N is composed of Li^+ and N^{3-} ions. Masdupuy (1957) reported ionic conductivity with an activation enthalpy of 0·53 eV, in agreement with the ionic model. However, the crystals have a ruby red colour, whereas ionic crystals should be colourless or white. Furthermore, the structure shows strongly directed bonds. These crystal properties support the covalent bonding of Li_3N suggested by Krebs (1968) and Suchet (1961). Krebs (1968) proposed bonding in the Li_2N layers by sp^2 hybrid functions of the Li atoms and the *p* orbitals of the N atoms. The sp^2 hybrid functions of the Li atoms overlap with two *p* orbitals of the N atoms as shown in Fig. 2(*a*). There are three different orientations of two *p* orbitals, which together form resonant Li–N bonds. The Li atoms of the N-free layers form *sp* hybrid functions parallel to **c** which overlap with the p_z orbital of the N atoms. In this bonding model all Li atoms are covalently bonded. Suchet (1961) assumed that all N and half of the Li atoms of a Li_2N layer form sp^2 hybrid functions which overlap as shown in Fig. 2(*b*). The remaining Li atoms appear as Li^+ ions. There are two different orientations of this arrangement which together form the resonant bonding system in these layers. Suchet (1961) proposed the same bonding type as Krebs (1968) for the Li–N bonds perpendicular to these layers.

Some NMR studies have supplied additional information. However, they could not resolve the problem of the nature of the chemical bond in this compound. The results of Bishop, Ring & Bray (1966) referred to the covalent bonds and to a diffusion of Li atoms above −75 °C. The diffusion was assigned to the atoms forming Li layers at $z = \frac{1}{2}$. A rather high jump frequency of 10–100 kHz and an activation energy of 0·55 eV were derived from the NMR data for the diffusing Li atoms. Burkert, Fritz & Stefaniak (1970) found that some of the Li atoms can be replaced by Mg atoms. Mg atoms occupy Li and additional sites in the N-free layers. Hendrickson & Bray (1973) reported long-range diffusion of the Li atoms with an activation energy of 0·57 eV.

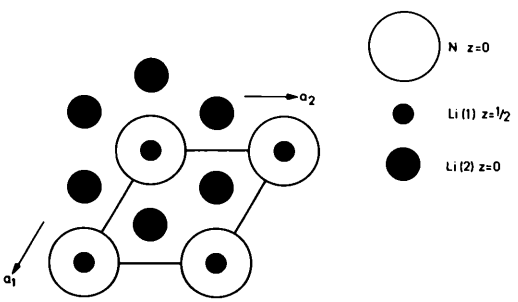

Fig. 1. Projection of the Li_3N structure along **c**.

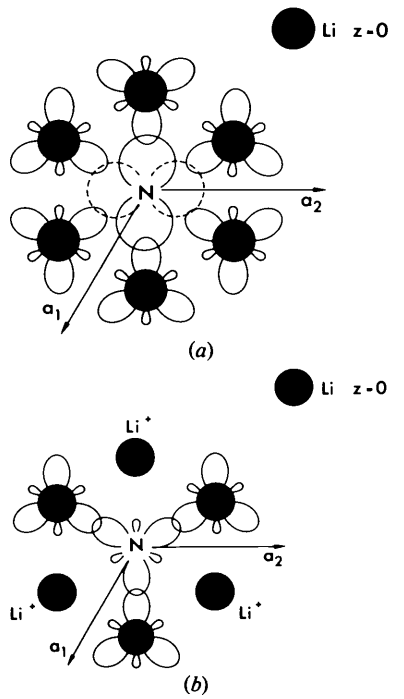

Fig. 2. Schematic drawings of two concepts for covalent bonds in the Li_2N layers at $z = 0$. (*a*) Covalent bonds are formed by overlapping sp^2 hybrid functions of the Li atoms with two *p* orbitals of the N atoms. The three different orientations of the *p* orbitals form the resonant Li–N bonds (Krebs, 1968). (*b*) Covalent bonds between half the Li atoms and the N atoms are formed by overlapping sp^2 hybrid functions. The remaining Li atoms appear as Li^+ ions. The two different orientations of this bonding scheme form the resonant Li–N bonds (Suchet, 1961).

Recently the ionic conductivity has been examined, both for polycrystalline samples (Bourkamp & Huggins, 1976) for which an activation energy of 0·61 eV was found, and for single-crystal samples (Alpen, Rabenau & Talat, 1977). For the latter, up to 300 °C, the Li conductivity perpendicular to **c** (the highest Li conductivity reported so far) is two orders of magnitude greater than that parallel to **c**, with activation enthalpies of 0·29 eV perpendicular to and 0·49 eV parallel to **c** respectively.

Furthermore it was concluded, from optical measurements and lattice-dynamical considerations, that Li_3N has an ionic configuration with the nitrogen ions close to the anomalous N^{3-} state (Chandrasekhar, Bhattacharya, Migoni & Bilz, 1978). Dielectric measurements at low temperatures showed that there exists a locally ionic motion in shallow potentials (Wahl & Holland, 1978). A survey of these and other new results on Li_3N is given by Rabenau (1978).

Thus the question of the nature of the bonding in Li_3N is still open. In the present paper this problem is investigated on the basis of X-ray diffraction data. In order to assess the ionic model, new atomic form factors for N^{3-} have been used. The details of the calculation are given in Schwarz & Schulz (1978). The structure investigation has been carried out once for covalent Li^0 and N^0 and once for ionic Li^+ and N^{3+} configurations.

2. Experimental

The two crystals used (with diameters of about 300 μm) were grown by the Czochralski technique (Schönherr, Müller & Winkler, 1978). The crystals were enclosed in an evacuated Lindemann-glass tube to prevent reaction with atmospheric moisture. The reflection intensities were measured with monochromated Mo $K\alpha$ radiation on a four-circle diffractometer in the θ–2θ mode. All reflections with $\sin\theta/\lambda \leq 1{\cdot}1$ Å^{-1} were scanned. The very low absorption correction factors (mass absorption factor $\mu = 0{\cdot}65$ cm^{-1}) and the path lengths of the X-rays were calculated by Gaussian integration with the crystal form described by its faces. The set of symmetry-independent data contained 125 observed and three unobserved reflections. A reflection was considered as observed if $I > 3\sigma(I)$ [I: net intensity; $\sigma(I)$: standard deviation calculated from counting statistics].

The data were collected at room temperature with the first crystal and at −40 and −120 °C with the second. For these temperatures the following lattice constants were obtained by refinement of the crystal orientation from the angular position of 24 reflections: a = 3·649 (1), 3·646 (1), 3·641 (1) Å; c = 3·877 (1), 3·874 (1), 3·872 (1) Å. The corresponding interatomic distances can be calculated by Li(1)–N = $c/2$ and Li(2)–N = $a/\sqrt{3}$.

3. Structure refinements

A normal least-squares structure refinement seems to be a suitable tool for deciding whether the Li_3N crystal is predominantly ionic or whether it has a covalent character. Scattering curves corresponding to $Li_3^+N^{3-}$ or $Li_3^0N^0$ should be used for these calculations. However, there are two difficulties.

(1) Only scattering curves for Li^0, Li^+, N^0 and N^- are published [in this work these were taken from *International Tables for X-ray Crystallography* (1974) and Fukamachi (1971)]. No scattering curves for N^{3-} are available, since it is not a stable free ion. Therefore, as a first step we followed the usual procedure of estimating the scattering curve for N^{3-} by extrapolation from the data of N^0 and N^- using the equation

$$f_e(N^{3-}) = 3f(N^-) - 2f(N^0). \qquad (1)$$

(2) There are only a few reflections with $\sin\theta/\lambda < 0{\cdot}4$ Å^{-1}. These are the main carriers of information on the charge of the N atoms (Fig. 3), since for larger $\sin\theta/\lambda$ values the scattering curves for N^{3-} and N^0 coincide almost completely. For the same reason it is impossible to obtain any information about the charge of the Li atoms, since the scattering curves for Li^+ and Li^0 are almost identical, even for the 001 reflection (Fig. 3).

In spite of these difficulties three different structure refinements were carried out using all F_o values or using only those F_o values with $\sin\theta/\lambda < 0{\cdot}65$ Å^{-1} or $\sin\theta/\lambda \geq 0{\cdot}65$ Å^{-1}. The isotropic extinction factor (Larson, 1967), the anisotropic temperature factors and the occupation probabilities of the Li atoms were refined. The weights for these and all other refinements were calculated with the standard deviations derived from the counting statistics. The corresponding R values, extinction factors and occupation probabilities are listed in Table 1 for the −40 °C data. Similar results were obtained with the other two data sets.

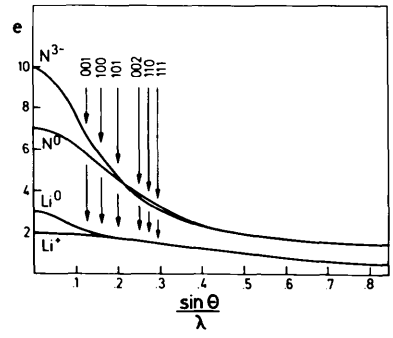

Fig. 3. Atomic scattering curves of N and Li. The arrows point to the $\sin\theta/\lambda$ values for reflections in Li_3N with $\sin\theta/\lambda < 0{\cdot}3$. For N^{3-} the extrapolated scattering curve $f_e(N^{3-})$ according to equation (1) is shown.

Table 1. *R values, extinction coefficients and occupation probabilities of the data set measured at −40 °C*

R and *R*(*W*) mean unweighted and weighted *R* values respectively. Three refinements were carried out for each set of scattering curves: all data, low-angle data only, and high-angle data only. For N^{3-} both the extrapolated scattering curve $f_e(N^{3-})$ and the scattering curve $f_W(N^{3-})$ for the optimum Watson radius $r_W = 1{\cdot}39$ Å were used.

Assumed charge	F_o values used	R	$R(w)$	Extinction coefficient ($\times 10^3$)	Occupation probability for Li(1) (0,0,$\frac{1}{2}$)	Occupation probability for Li(2) ($\frac{1}{3}$,$\frac{2}{3}$,0)
Li^0N^0	All sin θ/λ	0·020	0·028	−1·77 (27)	0·93 (1)	0·93 (1)
	sin $\theta/\lambda < 0{\cdot}65$	0·039	0·048	−2·9 (1·2)	0·94 (4)	0·90 (5)
	sin $\theta/\lambda \geq 0{\cdot}65$	0·011	0·010	–	1·01 (3)	0·99 (2)
Li^+N^{3-} $f_e(N^{3-})$	All sin θ/λ	0·011	0·012	0·47 (9)	0·962 (5)	0·959 (4)
	sin $\theta/\lambda < 0{\cdot}65$	0·009	0·011	0·29 (20)	0·97 (1)	0·95 (1)
	sin $\theta/\lambda \geq 0{\cdot}65$	0·013	0·012	–	0·99 (3)	0·96 (2)
Li^+N^{3-} $f_W(N^{3-})$ $r_W = 1{\cdot}39$ Å	All sin θ/λ	0·008	0·009	0·48 (7)	0·998 (4)	0·989 (3)
	sin $\theta/\lambda < 0{\cdot}65$	0·005	0·006	0·38 (10)	0·999 (5)	0·989 (6)
	sin $\theta/\lambda \geq 0{\cdot}65$	0·014	0·012	–	1·03 (3)	1·00 (2)

The results show the following inconsistencies, if neutral-atom scattering curves are used.

(1) The high-order refinement points to a nearly completely ordered Li distribution, but the refinements with all data, or with the low-angle data alone, show a reduction of the Li occupation probability of about 0·07.

(2) The *R* values are considerably higher for the low-angle data than for the high-angle data, in contrast to the expectation from counting statistics.

(3) The extinction coefficients become negative.

These discrepancies are removed to a large extent in the refinements using the Li^+ and the extrapolated N^{3-} scattering curves (Table 1). The Li positions now seem to be incompletely occupied with a deficiency of about 3%. These results suggest that bonding in Li_3N is ionic.

In the preceding paper (Schwarz & Schulz, 1978) new scattering curves for N^{3-} were reported. For these calculations the unstable N^{3-} ion was stabilized by an external potential. This potential is produced by a charge of +3 e uniformly distributed over the surface of a sphere, a concept first introduced by Watson (1958). The scattering curves denoted in the following by $f_W(N^{3-})$ are critically dependent on the radius of the sphere, r_W, and are tabulated in the preceding paper as a function of r_W. The structure refinements for the three sets of data were repeated using the new scattering curves. The weighted $R(w)$ values, isotropic extinction factors and occupation probabilities from these refinements are shown as a function of r_W in Fig. 4.*

The weighted $R(w)$ curves obtained show minima for r_W between 1·32 and 1·46 Å for all three temperatures

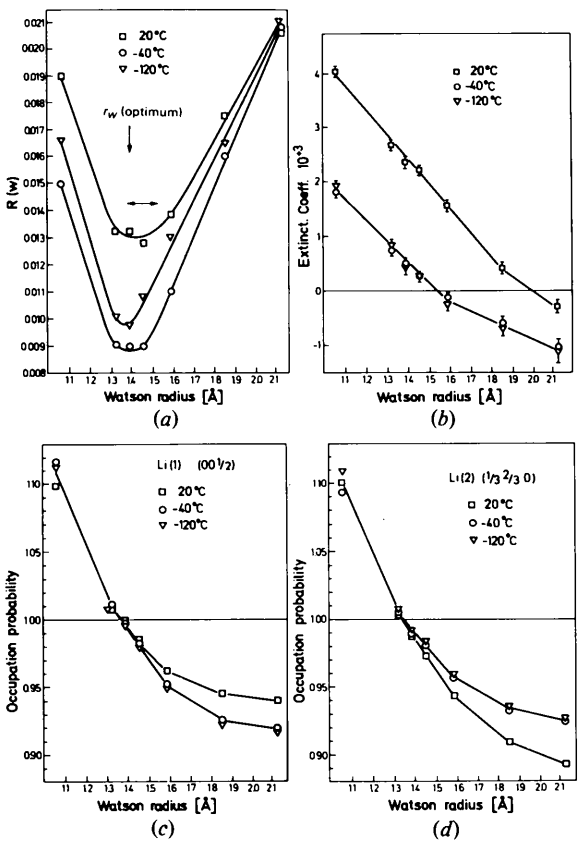

Fig. 4. Essential results of the refinements (Li^+ and N^{3-} being assumed) using the scattering curves $f_W(N^{3-})$ for different Watson radii. (*a*) Weighted *R* values: $R(w) = [\sum w(F_o - F_c)^2/\sum wF_o^2]^{1/2}$. The higher $R(w)$ value at −120 °C (compared with that at −40 °C) is caused by a larger temperature instability of the cooling equipment at lower temperatures. (*b*) Isotropic extinction coefficient. The error bars correspond to the standard deviations. (*c*) Occupation probability of Li(1). The standard deviations are smaller than the symbols. (*d*) Occupation probability of Li(2).

* Lists of structure factors at the three temperatures studied here have been deposited with the British Library Lending Division as Supplementary Publication No. SUP 33716 (4 pp.). Copies may be obtained through The Executive Secretary, International Union of Crystallography, 5 Abbey Square, Chester CH1 2HU, England.

Table 2. *Structure parameters at* −120, −40 *and* 20 °C *using the scattering curve* $f_W(N^{3-})$ *for* $r_W = 1{\cdot}39$ Å

The U values are multiplied by 100. From the point symmetry of the atomic positions: $U_{11} = U_{22} = 2U_{12}$; $U_{13} = U_{23} = 0$. The anisotropic temperature factor is defined in the form: $T = \exp\left(-2\pi^2 \sum_{i,j=1}^{3} U_{ij} h_i h_j a_i^* a_j^*\right)$.

	Atomic position (Wyckoff notation)	U_{ij} (Å² × 10²)				Occupation probabilities	
			−120 °C	−40 °C	+20 °C	−120 °C	−40 °C	20 °C
N	1(*a*)	U_{11}	0·622 (9)	0·775 (6)	0·929 (9)			
		U_{33}	0·585 (12)	0·775 (9)	0·950 (12)			
Li(1)	1(*b*)	U_{11}	1·25 (2)	1·60 (1)	1·89 (3)	0·997 (5)	0·998 (4)	1·003 (4)
		U_{33}	0·71 (3)	0·86 (2)	1·07 (4)			
Li(2)		U_{11}	0·88 (1)	1·08 (2)	1·26 (2)	0·990 (5)	0·989 (3)	0·982 (4)
		U_{33}	1·81 (3)	2·48 (2)	3·07 (4)			

(Fig. 4*a*). The extinction factors and the occupation probabilities of the two Li positions are also strongly r_W-dependent (Figs. 4*b–d*). From Fig. 4 one can exclude r_W values leading to physically meaningless results: extinction factors lower than zero or occupation probabilities larger than one. There remains only a small range of r_W between 1·38 and 1·53 Å (marked by a double arrow in Fig. 4*a*). Obviously, this range would be smaller still if crystals without extinction had been available. The scattering curve for $r_W = 1{\cdot}39$ Å gives the best overall results and has been used for all calculations and considerations described below.

The occupation probabilities and coefficients of the anisotropic temperature factors of the three data sets are listed in Table 2 for the optimum r_W value. In addition, the results of the high- and low-order refinements with the −40 °C data are included in Table 1. No discrepancies are now observable between these refinements. The Li(1) position is fully occupied, but the Li(2) position shows an under-occupation of 1–2% at all investigated temperatures (Table 2).

4. Electron density difference syntheses

The deviations from a purely ionic-bonded crystal were studied by difference syntheses as follows.

(1) The N^{3-} scattering curve for the optimized value of r_W and the Li^+ scattering curve were used. The occupation probabilities were taken from Fig. 4(*c*) and (*d*) for the optimized r_W value and applied to all three data sets [1·00 for Li(1) and 0·99 for Li(2)]. In the same way the extinction correction factor was taken from Fig. 4(*b*).

(2) The temperature factors were refined using only F_o values with $\sin\theta/\lambda \geq 0{\cdot}65$ Å^{-1}. These temperature factors were somewhat lower than those obtained from the refinements with all data (Table 2), but the differences were smaller than the e.s.d.'s.

(3) The scale factor was determined by a structure factor calculation with all data to account for thermal diffuse scattering in an approximate way (Vos, 1977).

In the difference syntheses calculated with the above data only electron densities up to 0·1 e Å^{-3} were

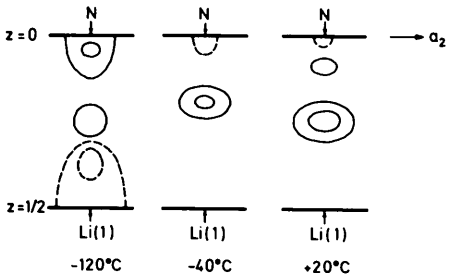

Fig. 5. Difference electron densities along the Li(1)–N bond at −120, −40 and 20 °C. Full and broken lines correspond to positive and negative densities respectively. The lines are drawn at |0·05| and |0·10| e Å^{-3}.

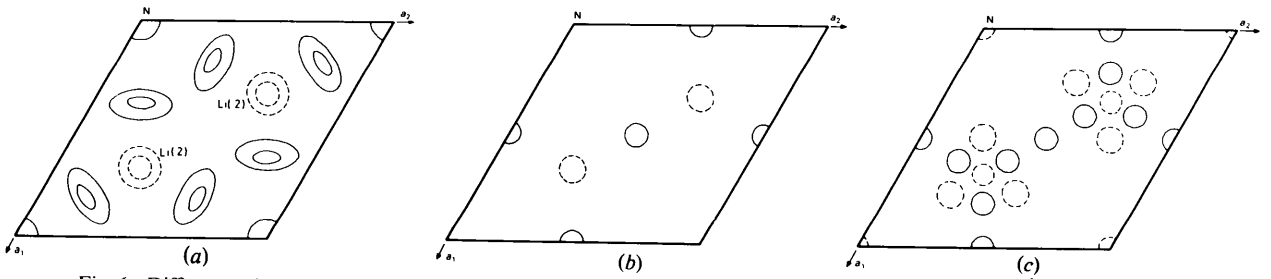

Fig. 6. Difference electron densities in the Li_2N plane at $z = 0$. Details are as in Fig. 5. (*a*) −120 °C. (*b*) −40 °C. (*c*) 20 °C.

observed. Their estimated error is roughly 0·03 e Å^{-3}, if the e.s.d.'s of the measured reflections and similar e.s.d.'s for the unmeasured reflections are taken into account. Since the maximum densities in these difference syntheses are only about three times larger than their e.s.d.'s, this suggests that there is only a small deviation from pure ionic bonding. In Fig. 5 the residual electron densities along the Li(1)–N bond, *i.e.* along **c**, are shown. The only common feature for the three temperatures studied is a small amount of electron density approximately in the middle of the bond. This density may be interpreted as a polarization of the N^{3-} electron cloud in the Li(1) direction. The residual electron densities in the Li_2N plane around the Li(2) positions at −120 °C (Fig. 6*a*) can be interpreted in the same way, although these densities disappear at −40 °C (Fig. 6*b*). The positive and negative densities around this position at room temperature indicate anharmonic thermal vibrations which are not included in the present structure refinements. The negative electron densities at the Li(2) position at all temperatures suggests that the occupation probability of Li(2) lies between 0·99 and 0·98.

5. Model calculations

It could be argued that the small Li^+ ions would influence the rather diffuse spherical N^{3-} ions and at least generate anisotropic polarization effects. However, such effects are hardly observable in the residual electron densities of Figs. 5 and 6. It may be possible that such polarization effects would not be observed in the difference densities for the following reasons.

(1) With decreasing volume V of an elementary cell, the first term of the Fourier summation $F(000)/V$ increases and the modulation of this term by the structure factors decreases. This argument will be particularly cogent for Li_3N, owing to the small lattice constants of the crystal.

(2) The procedure of optimizing the N^{3-} scattering curves by varying r_W, rather than using a fixed scattering curve (here used for the first time), could result in the isotropic contribution to the electron density being over-emphasized, and cause a nearly perfect adjustment of the 'wrong' purely ionic model to an anisotropic electron density distribution around the N^{3-} ions. Thus its residual anisotropic electron densities may be so small that they become comparable with the errors of the difference densities.

In order to assess the importance of these two effects, we have made a model calculation in which the electron density of N consists of an isotropic and an anisotropic part. It was assumed that the true electron distribution in Li_3N can be described as follows: The Li positions are occupied by Li^+. The isotropic part of the N^{3-} ions is represented by N^0. The remaining three electrons generate the anisotropic part. They are uniformly distributed among the eight Li–N bonds. These fractional electron densities ($\frac{3}{8}$ e) were placed in the middle of the Li–N bonds and smeared by an isotropic temperature factor of $B = 10$ Å^2. The middle of these densities is about 1·1 Å from the Li and N positions; this means that it lies outside the Li^+ and N^0 radii, but inside the lower limit of the N^{3-} ionic radius. The temperature factors for Li^+ and N^0 were taken from the −40 °C values of Table 2. The structure factors obtained from the above model were taken as hypothetical F_o values and used for refinements with the different N^{3-} scattering curves. The best fit produced an R value of $R(w) = 0{\cdot}034$.

A difference density was now calculated with the correct temperature factors of Li^+ and N^0 (this corresponds to a high-order refinement) and an adjusted scale factor. This difference synthesis (Fig. 7) clearly shows the artificial polarization densities and, in addition, a large negative density at the N position. Thus it is possible to conclude that any anisotropic term in the electron density of Li_3N would readily be observed in a difference synthesis employing ionic scattering curves only.

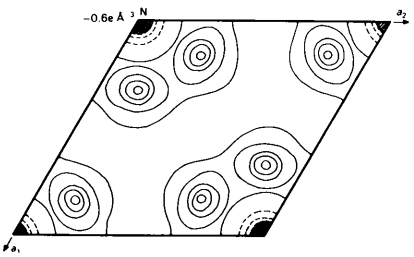

Fig. 7. Difference density between a model electron density (see text) and the best fit to it by a pure ionic structure ($Li_3^+N^{3-}$). The full and broken lines show positive and negative electron densities, respectively, and are drawn at |0·05|, |0·10|,... e Å^{-3}.

6. Discussion

In the previous sections it was shown that both the extrapolated scattering curve $f_e(N^{3-})$ and the $f_W(N^{3-})$ curves indicate that Li_3N is an ionic crystal containing the N^{3-} ion. For the first time the existence of an N^{3-} ion has been proved by diffraction methods. An ionic radius for N^{3-} is estimated to be $r(N^{3-}) = 1{\cdot}5$ Å by subtracting the Li^+ radius $r(Li^+) = 0{\cdot}6$ Å from 2·1 Å, the average interatomic Li–N distance in Li_3N. Although both types of refinements which assume ionic configuration give low R values of about 1%, the structural parameters obtained differ considerably. The extrapolated scattering curve $f_e(N^{3-})$ indicates an under-occupation of both Li sites by about 3% and a nearly extinction-free crystal (Table 1). A more reliable

answer to the question of occupational disorder can only be obtained by using a series of $f_W(N^{3-})$ scattering curves for the structure refinements. They show the strong dependence of all structure parameters on the Watson radius r_W (see Fig. 4). This also holds for the temperature factors which are not discussed in this paper. There exists a small range of r_W for which consistent results are obtained and within this range there exists an optimum r_W value which gives the overall best fit to the observed data. For this optimum r_W value the occupation probabilities of the Li sites can be taken from Fig. 4(*c*) and (*d*) with an error lower than 1%. Within this error limit the Li(1) sites at $z = \frac{1}{2}$ are completely ordered, whereas the Li(2) sites at $z = 0$ show a weak under-occupation in the range of 1–2% (Tables 1 and 2 and Fig. 4).

From the point of view of ionic conduction the following observations can be made.

(1) The Li^+ ions within the Li_2N layers [Li(2)] are more weakly bonded to the N^{3-} ions than are the Li^+ forming the Li layers [Li(1)], as indicated by the interatomic distances [Li(1)–N = 1·94, Li(2)–N = 2·13 Å] and by the thermal-vibrational amplitudes (Table 2). Therefore, Li(2) should play a preferred role in the ionic conduction of Li_3N.

(2) From the NMR results mentioned in § 1 it was deduced that mainly the Li(1) positions contribute to the ionic conduction.

(3) Refinements with the extrapolated N^{3-} scattering curve [$f_e(N^{3-})$] produce an under-occupation at *both* Li sites of about 3%.

(4) Refinements with the $f_W(N^{3-})$ scattering curves resulted in completely ordered Li(1) sites and an under-occupation of the Li(2) sites of about 1–2%.

Results (2) and (3) do not exclude each other, although they are in contradiction to (1) and (4). Only (1) and (4) agree and support each other. This correspondence makes it probable that only the Li(2) sites are involved in ionic conduction. The different conclusions reached in (3) and (4) again show how sensitive the structure refinements are to the scattering curves used.

We thank Professors H. Bilz and A. Rabenau for their stimulating interest in this work and for many helpful discussions; we also thank Dr E. Schönherr and G. Müller for growing the crystals and K. H. Thiemann for assistance during data collection. (All are at the Max-Planck-Institut für Festkörperforschung, Stuttgart.)

References

ALPEN, U. VON, RABENAU, A. & TALAT, G. H. (1977). *Appl. Phys. Lett.* **30**, 621–623.

BISHOP, S. G., RING, P. J. & BRAY, P. J. (1966). *J. Chem. Phys.* **45**, 1525–1531.

BOURKAMP, B. A. & HUGGINS, R. A. (1976). *Phys. Lett. A*, **58**, 231–233.

BRILL, R. (1927). *Z. Kristallogr.* **65**, 93–99.

BURKERT, P. K., FRITZ, H. P. & STEFANIAK, G. (1970). *Z. Naturforsch. Teil B*, **25**, 1220–1225.

CHANDRASEKHAR, H. R., BHATTACHARYA, G., MIGONI, R. & BILZ, H. (1978). *Phys. Rev. B*, **17**, 884–893.

FUKAMACHI, T. (1971). *Mean X-ray Scattering Factors Calculated from Analytical Roothaan–Hartree–Fock Wave Functions by Clementi Methods*. Tech. Rep. B12, p. 24. Tokyo: Institute for Solid State Physics.

HENDRICKSON, J. D. & BRAY, P. J. (1973). *J. Magn. Reson.* **9**, 341–357.

International Tables for X-ray Crystallography (1974). Vol. IV, pp. 155–173. Birmingham: Kynoch Press.

KREBS, H. (1968). *Grundzüge der anorganischen Kristallchemie*, pp. 247–248. Stuttgart: Ferdinand Enke Verlag.

LARSON, A. C. (1967). *Acta Cryst.* **23**, 664–665.

MASDUPUY, E. (1957). *Ann. Chim. (Paris)*, **2**, 527–586.

RABENAU, A. (1978). *Festkörperprobleme*. Vol. XVIII, pp. 77–108. Braunschweig: Pergamon/Vieweg.

RABENAU, A. & SCHULZ, H. (1976). *J. Less-Common Met.* **50**, 155–159.

SCHÖNHERR, E., MÜLLER, G. & WINKLER, E. (1978). *J. Cryst. Growth.* **43**, 467–472.

SCHWARZ, K. & SCHULZ, H. (1978). *Acta Cryst.* A**34**, 994–999.

SUCHET, J. P. (1961). *Acta Cryst.* **14**, 651–659.

VOS, A. (1977). Personal communication.

WAHL, J. & HOLLAND, U. (1978). *Solid State Commun.* **26**, 229–233.

WATSON, R. E. (1958). *Phys. Rev.* **111**, 1108–1110.

ZINTL, E. & BRAUER, G. (1935). *Z. Elektrochem.* **41**, 102–107.